02

A criterion for determination of the upper critical fields H_{c2} in YBCO thin films with different ion irradiation doses

© A.V. Antonov[1], D.V. Masterov[1], A.N. Mikhaylov[2], S.V. Morozov[1], S.A. Pavlov[1], A.E. Parafin[1], D.I. Tetelbaum[2], S.S. Ustavschikov[1,2], P.A. Yunin[1,2], D.A. Savinov[1,2,¶]

[1] Institute of Physics of Microstructures, Russian Academy of Sciences, Nizhny Novgorod, Russia
[2] Lobachevsky State University, Nizhny Novgorod, Russia

¶ E-mail: savinovda@ipmras.ru

Received April 17, 2023
Revised April 17, 2023
Accepted May 11, 2023

Magnetotransport measurements were carried out for $YBa_2Cu_3O_{7-x}$ (YBCO) thin films in external perpendicular magnetic fields of H. The studies were performed both for the virgin samples and for the irradiated ones. Xenon ions were used as an external irradiation. Thus we studied features of the broadening of superconducting transition in YBCO films (virgin and irradiated). The broadening of superconducting drop was analyzed depending on an external magnetic field H, as well as on an irradiation dose n_D. When processing the experimental data $R(H, T)$, we studied a criterion for determination of temperature dependence of the upper critical field $H_{c2}(T)$. The criterion was analyzed depending on the defect concentration in the film corresponding to a certain value of n_D. It was found out that for a virgin sample, H_{c2} should be determined by the resistance level $R = 0.4R_N$ inside the superconducting transition, where $R_N = R(T = 100\,\mathrm{K})$. With a gradual increase in n_D, this resistance level decreases. At sufficiently high radiation doses $n_D > 7 \cdot 10^{12}\,\mathrm{cm}^{-2}$, the $H_{c2}(T)$ phase transition line should be determined by the level $R \approx 0$.

Keywords: thin films, HTSC, xenon ion irradiation, magnetotransport studies, broadening of the superconducting transition, upper critical field, phase transition line, Tinkham's formula, Abrikosov vortices.

DOI: 10.21883/PSS.2023.06.56093.23H

1. Introduction

The transition to the superconducting state is the second-order phase transition [1]. On the plane external magnetic field H — temperature T, the phase transition line between normal and superconducting phases is described by the temperature dependence of the upper critical field $H_{c2}(T)$. From a theoretical point of view, the transition to the superconducting state should lead to a sharp disappearance of the resistance R. However, looking at typical experimental data from transport measurements, it should be noted that there is no abrupt reduction R to zero. Resistive transitions $R(T)$ are always broadened, especially in the presence of an external magnetic field H. Usually, the broadening is a consequence of the motion of Abrikosov vortices, namely their creep and flow (see [2] and [3], respectively). The superconducting transition broadening can also be explained by other mechanisms — spatial heterogeneity (e.g., changing in the critical temperature T_{c0} [4]), superconducting fluctuations [5], the occurrence of surface superconductivity [6], competition between different types of localized superconducting order parameter nucleation in the magnetic field H [7]. The possible presence of all these mechanisms in magnetic transport measurements leads to an ambiguous interpretation of the superconducting transition broadening. This circumstance makes it impossible to determine the fundamental parameters of superconductivity, such as superconducting coherence lengths, because it is not clear what exactly the resistance inside the superconducting transition corresponds to $H = H_{c2}$. The following criteria R are often used to determine the upper critical fields: $R = 0.1R_N$, $R = 0.5R_N$, $R = 0.9R_N$, where R_N — resistance in normal state (see e.g. papers [8–10]). In some cases, the criterion on R can be arranged in more complex ways. In particular, this has been demonstrated in paper [11]. The authors studied the typical resistance R inside the superconducting transition, which defines the phase transition line $H_{c2}(T)$ in highly disordered In/InO_x thin-film superconductors with a critical temperature of $T_{c0} \approx 2\,\mathrm{K}$. Within the framework of the two-dimensional Aslamazov-Larkin theory, they defined a criterion $R = (0.3-0.4)R_N$, which depends on the film thickness and the degree of disorder. Here, we want to emphasize that a detailed study of the relevant criterion for H_{c2} is necessary for any superconducting sample, especially for disordered compounds. The case of high-temperature superconductors (HTSC) deserves special attention. One of the most intriguing superconducting properties of these materials is their extremely high upper critical field values H_{c2}. The superconducting transition in HTSC has a significantly non-uniform broadening in the magnetic field H — the upper part of the transition has a much weaker dependence on H than in the area near the bottom, where $R \approx 0$. This, together with the

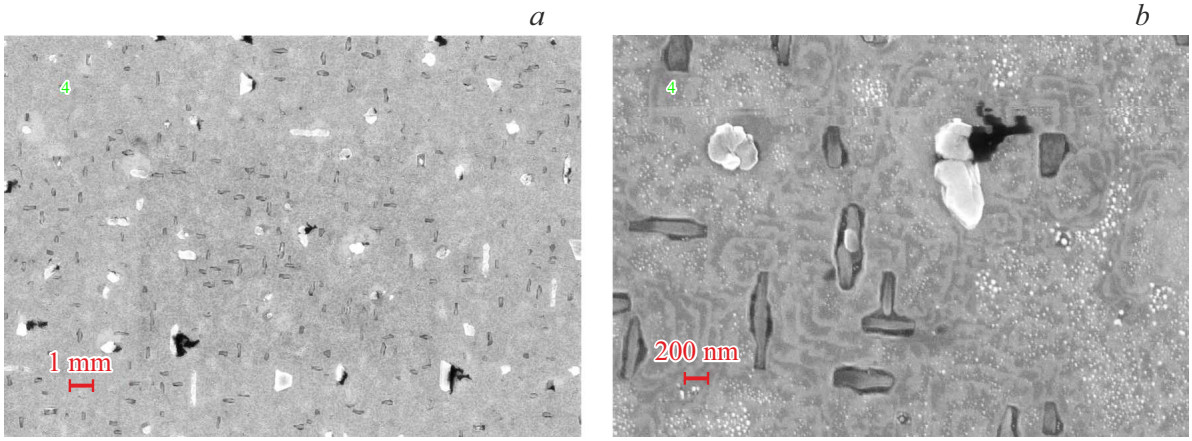

Figure 1. Secondary electron image of the surface of the YBCO film under study obtained with a scanning electron microscope (SEM).

high values of H_{c2}, makes the experimental determination of H_{c2} in such materials extremely difficult. As a consequence, values $H_{c2}(0)$, estimated within different theoretical models (e.g. based on the Werthamer model [12]), may widely vary depending on one or the other criterion on the resistance R inside the superconducting transition.

In the present paper, we have studied the features of superconducting transition broadening in HTSC in strong magnetic fields H. Namely, we performed magnetic transport measurements of the resistance $R(H, T)$ in plane (ab) for YBCO epitaxial thin films. Based on the theoretical Tinkham model [13], we have studied the resistance value R^*, which separates the superconducting transition broadening caused by vortex motion from the broadening caused by the other mechanisms mentioned above. Obviously, this is exactly the resistance level on the series of resistance curves $R(H, T)$, which corresponds to H_{c2}. Indeed, the transition from superconducting to normal state is the second-order phase transition and therefore occurs smoothly when the external parameters change (H and/or T), rather than in an abrupt way. This transition is associated with a gradual increase in the concentration of vortices, which begin to overlap their normal cores at $H = H_{c2}$. The lower part of the superconducting transition ($0 < R < R^*$) is determined by the features of the vortex motion (their creep and flow). In this paper, we study in detail the determination of value R^* for virgin YBCO films as well as for the films irradiated with xenon ions at an energy of 150 keV. The irradiation was carried out in several stages. Each stage was characterized by a total accumulated dose n_D. The irradiated sample possessed a rather more smearing superconducting transition in a zero magnetic field than a virgin sample. The broadening became more pronounced with increasing n_D. This created an additional difficulty in the determination of the phase transition line. However, we have analyzed the effect of disorder on R^* and formulate a criterion for the determination of H_{c2} fields for a wide range of doses n_D.

2. Sample and ion irradiation

In the present paper, we studied the high-quality c-epitaxial oriented YBCO films with a thickness of $d = 50$ nm (axis c is perpendicular to the substrate surface). $LaAlO_3$ lanthanum aluminate with crystal-lattice orientation (001) was used as a substrate. Fig. 1 shows an image of the film surface obtained using a scanning electron microscope (SEM). Transport measurements were carried out using a standard four-probe technique. Different bridges were obtained using the ion irradiation through a photoresist mask, which was then removed in acetone. Virgin bridges had different dimensions, but the same width/length ratio 1/5. The contact pads were fabricated by thermal spraying of silver through a metal mask. The silver layer was 100 nm thick. Critical temperature $T_{c0} = 89$ K, critical current density $j_c = 4 \cdot 10^6$ A/cm^2 at $T = 77$ K. The calculated resistivity of each bridge at temperature $T = 100$ K was $100\,\mu\Omega \cdot$ cm, which corresponds to the optimum of oxygen doping of the film, i.e. the value $x = 0.1$ in $YBa_2Cu_3O_{7-x}$. In our study, we used a bridge with the following dimensions: width 50 μm, length 250 μm (see Fig. 2).

Note, that the surface morphology of the film is imperfect — it contains many structural defects with characteristic sizes in the range from a few nm to hundreds nm (see typical SEM images of the film surface in Fig. 1). The largest visible defects are called second-phase precipitates (see light and dark inclusions). These are usually copper and yttrium oxides. However, as can be seen from Fig. 1, the average distance between them significantly exceeds their characteristic size, and the superconducting transition in zero magnetic field appears to be rather narrow — about 1 K (see below). So, the sample can be considered as a quasi-homogeneous film with a given

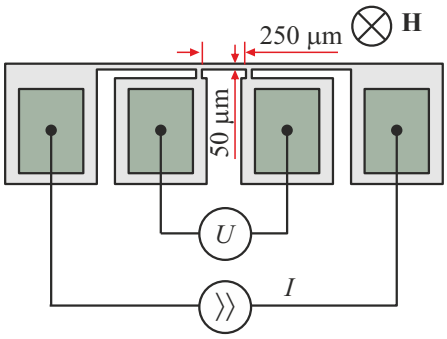

Figure 2. Schematic image of the bridge under study.

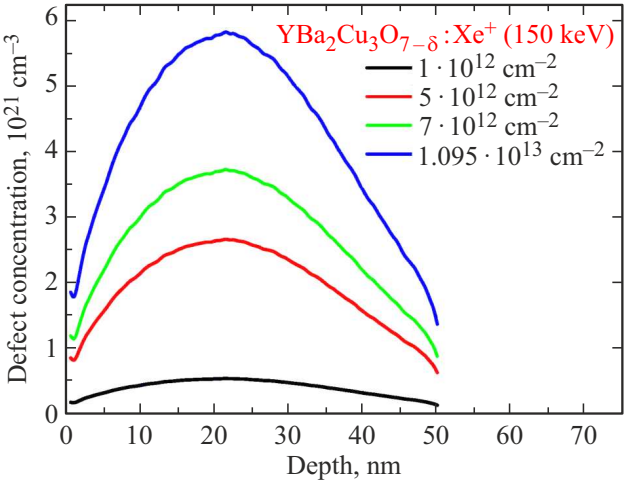

Figure 3. Depth distribution of the defect concentration for different irradiation doses n_D shown in the insert.

critical temperature T_{c0} and a certain distribution of vortex pinning centers. Such a consideration appears to be a basis for the theoretical description of the experimental resistance dependencies $R(H, T)$, which will be presented in the following sections.

To create a sample with a certain defect concentration, we carried out irradiation at room temperature with xenon ions (Xe^{2+}) at an energy of 150 keV. The choice of Xe^{2+} ions is due to the fact that it is chemically inactive and the mass of the xenon atom significantly exceeds the atomic masses of all the elements making up the film. In this case, the deviation of the ion trajectory from the normal is relatively small and the disordered area created by each ion can be approximated by a cylinder with an axis perpendicular to the surface (see [14]). Several stages of ion irradiation were carried out, starting with an initial dose $n_D = 10^{12}$ cm^{-2}. As a result, the maximum accumulated dose was $n_D = 9.45 \cdot 10^{12}$ cm^{-2}. Fig. 3 shows the concentrations of irradiation-generated Frenkel pairs for different doses n_D, calculated using the SRIM code [15]. It can be approximated that each ion creates a quasi-cylindrical defect cluster with some characteristic cross section size (see [14] for typical estimates).

3. Experiment

The sample resistance was measured by a standard four-probe technique. The transport current was 1 μA. Resistive measurements were carried out with a magnetic field sweep up to 12 T in the temperature range from 100 K and lower. To create the magnetic field a closed-cycle cryogenic system of two cryostats was used, one of which contained a superconducting solenoid with a hole 52 mm in diameter (Oxford Cryofree SC magnet), and the second cryostat (Oxford Optistat PT) with controlled temperature (from 1.6 K and above) was inserted into this hole, where the test sample was located. The temperature T was determined by a special calibrated thermometer with a resolution of 50 mK. The magnetic field H was determined with a resolution 12 G.

Thus, for different fixed temperature values T, we found experimental dependencies of the resistance R in the plane (ab) on H for different doses n_D. Note, that to verify our measurements, we also chose a lower transport current value — 0.1 μA. No changes were found in dependencies $R(H, T)$, confirming the validity of our conclusions presented in the next section.

4. Results and discussion

We start this section with presentation of the dependencies of $R(T)$ corresponding to $H = 0$ and different doses of n_D (see Fig. 4). For given doses of n_D, the temperature dependence of the resistance R of the film corresponds to the behavior of a typical metal which possesses a superconducting transition. The superconducting transition

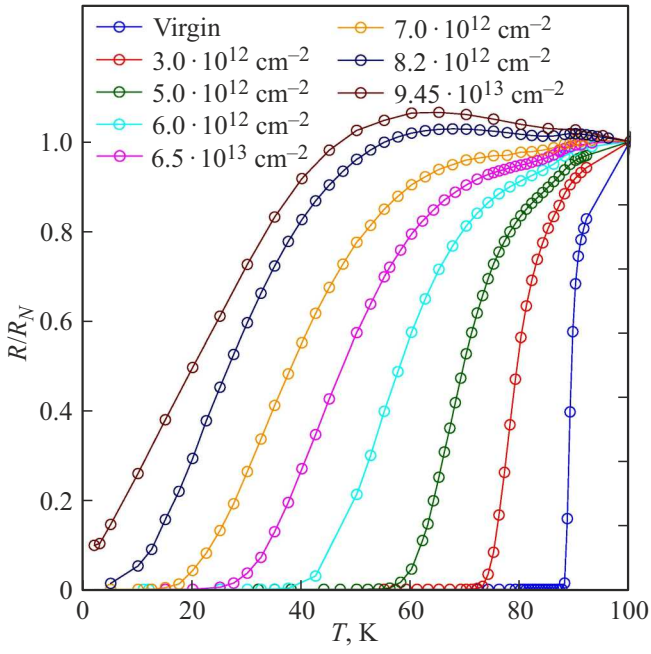

Figure 4. Experimental curves $R(T)/R_N$ for $H = 0$ and different values of n_D shown in the insert.

is broadened by increasing of n_D. All curves in Fig. 4 are presented for normalized values of $R(T)/R_N$. In this paper, we define $R_N = R(100\,\mathrm{K})$, as the beginning of the normal state. The normal state in YBCO is characterized by a known linear temperature dependence of resistance and negligible magnetoresistance. So, for $T = 100\,\mathrm{K}$ the dependence $R(H)$ is extremely weak in the considered range of external field values H: $R(H) \approx R_N = \mathrm{const}$ for each of n_D. We assume R_N as a reference value and different resistive curves in our manuscript will be presented in fractions of it. Obviously, the value of R_N depends on n_D. This dependence is shown in Fig. 5. Over a wide range of n_D values up to $5 \cdot 10^{12}\,\mathrm{cm}^{-2}$, the dependence $R_N(n_D)$ appears to be quasi-linear. The nonlinearity for higher doses may be related to the overlap of defect clusters arising during irradiation. Indeed, at such doses the lateral sizes of individual clusters appear comparable to the average distance between them (see discussion in [14]). Fig. 5 also shows the dependence $T_{c0}(n_D)$. A linear dependence of critical temperature on dose is observed up to $5 \cdot 10^{12}\,\mathrm{cm}^{-2}$; above this dose the dependence becomes non-linear, which may be due to overlapping of disordered areas.

As was mentioned in the introduction, the superconducting transition in HTSC has a significantly inhomogeneous broadening in the magnetic field H, with the upper part of the transition having a much weaker dependence on H than in the area near the bottom where $R \approx 0$. This feature can also be demonstrated in Fig. 6, which shows the experimental dependences $R(H)/R_N$ for different temperatures T inside the superconducting transition. Indeed, a strong magnetic field dependence of resistance is observed for rather low T and a weak field dependence $R(H)$ near temperatures close to the transition to the normal state. In this figure, we have separately presented curve $R(H)$ for $T = 100\,\mathrm{K}$ (marked in red) to identify the start of the

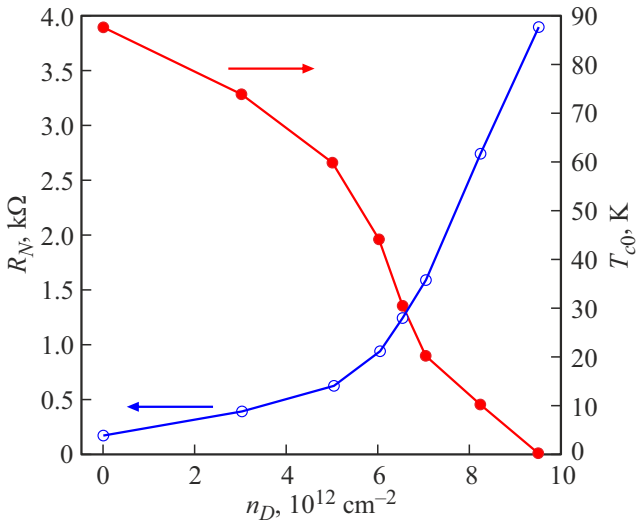

Figure 5. Dependencies of normal sample resistivity $R_N = R(100\,\mathrm{K})$ and critical temperature T_{c0} on irradiation dose n_D.

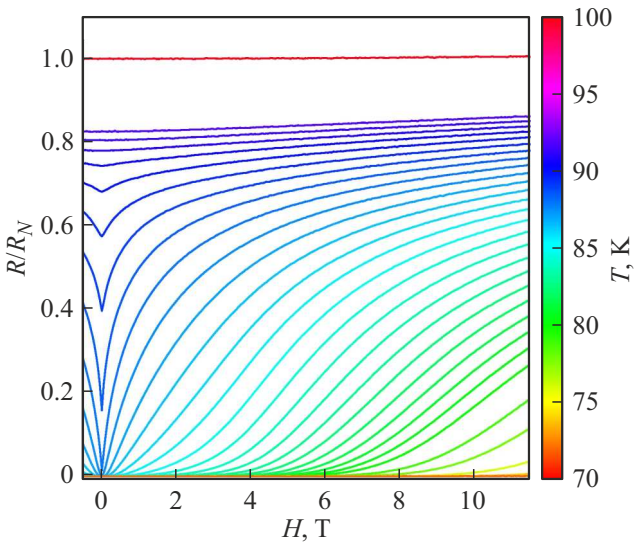

Figure 6. Experimental $R(H)/R_N$ curves for different T and $n_D = 0$ (virgin sample).

normal state. Due to the high values of H_{c2} in YBCO, the choice of one or the other criterion on R leads to a wide variation in the superconducting coherence length. In the present paper, we determine a value of $R = R^*$, which separates the superconducting transition broadening caused by vortex motion from the broadening caused by other mechanisms [4–6]. It is this resistance level R that corresponds to H_{c2}. The lower part of the superconducting transition ($0 < R < R^*$) is determined by the features of the vortex motion (their creep and flow). According to [13], this part of the superconducting transition in HTSC is described by the following formula:

$$R = R_N \cdot \left\{ I_0 \left[A(1 - T/T_{c0})^{3/2}/H \right] \right\}^{-2}, \qquad (1)$$

where I_0 — modified Bessel function, A — constant related to pinning properties in the superconductor. From formula (1), it is easy to see that for any chosen level R/R_N, the phase transition line $H(T)$ turns out to be non-linear near T_{c0}: $H(T) \propto (1 - T/T_{c0})^{3/2}$. This feature (typical for all HTSC) is known in the literature and is commonly referred to a positive curvature of the critical fields near T_{c0} (in particular, see the experimental data for YBCO in paper [16]). This behavior of $H(T)$ corresponds to rather small R, close to zero, and results in smaller critical values than the actual ones for a given material. This fact can be illustrated in Fig. 7, which shows typical dependencies $H(T)$ for different values of R/R_N — from 0.02 to 0.8. In Fig. 8, we separately show the experimental curve $H(T)$ for the value $R/R_N = 0.02$. This figure also shows the correlation

$$H(T) \propto (1 - T/T_{c0})^{3/2}, \qquad (2)$$

which should describe the phase transition line in some interval of magnetic fields for sufficiently low resistive levels,

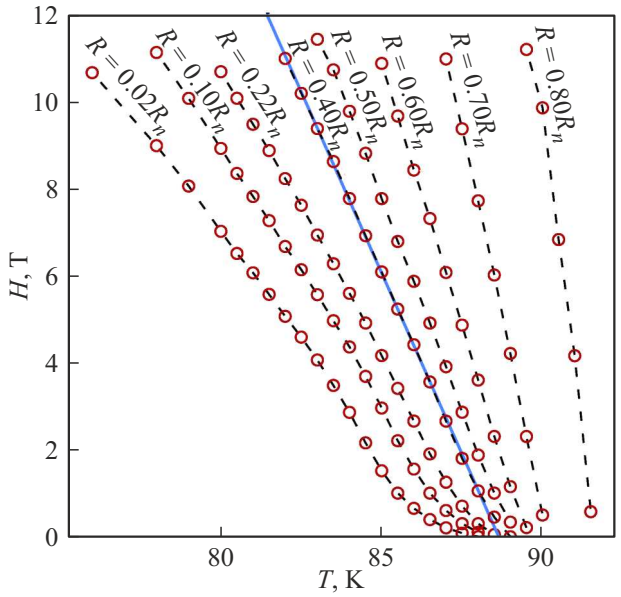

Figure 7. Dependencies $H(T)$ for different values of R/R_N and $n_D = 0$ (virgin sample). The symbols illustrate the experimental data and the dashed lines are obtained by spline interpolation. The solid blue line corresponds to a linear approximation over the set of experimental points represented by symbols for a given value R/R_N (the slope of this line corresponds to the slope of the critical field temperature dependence $H_{c2}(T)$).

as follows from formula (1). Note that for the magnetic fields $H < 4\,\mathrm{T}$, there is a good agreement between the experimental data and the theoretical approximation (2). Considering large values of R/R_N, a gradual trend towards a linear relationship $H(T)$ should be noted, as can be seen from Fig. 7. Therefore, for these dependencies $H(T)$, we obtain a good agreement between the experimental data and Tinkham's model for substantially lower magnetic fields H than in the case of $R/R_N = 0.02$. Note, that by increasing R to a value of $0.4R_N$, we obtain a quasi-linear dependence $H(T)$ (see Fig. 7). Obviously, this line cannot be described within Tinkham's model. Therefore, we argue that this is the line in the plane external magnetic field H — temperature T, which should be called by the line $H_{c2}(T)$. For larger values of R, the dependences $H(T)$ appear quasi-linear with different slope values (see lines corresponding to $R = 0.5R_N$, $R = 0.6R_N$, $R = 0.7R_N$, and $R = 0.8R_N$ in Fig. 7). Certainly, these dependencies cannot also be described within Tinkham's model. Thus, the broadening of the superconducting transition for the high resistances $(0.4R_N < R < R_N)$ is not due to the vortex effects. Thus, we find a criterion for the determination of the upper critical field for the virgin sample: $R^* = 0.4R_N$. Note, that the slope $dH/dT|_{T=T_{c0}}$, determined according to the condition $R^* = 0.4R_N$, and the value of the superconducting coherence length correspond to the known literature data on the study of epitaxial YBCO films (see, for example, [17]). In particularly, the coherence length in the plane (ab) is 1.6 nm.

Let us apply this approach to find lines $H_{c2}(T)$ for YBCO film with specific doses of ion irradiation n_D. Considering the cases of moderate doses — $n_D = 10^{12}\,\mathrm{cm}^{-2}$ and $n_D = 3 \cdot 10^{12}\,\mathrm{cm}^{-2}$, one can see the reduction in the critical temperature T_{c0} (see Fig. 4). The typical $R(H, T)$ curves appear to be similar to those shown in Fig. 6 for the virgin sample. Therefore, they are omitted here. Starting with a dose of $n_D = 5 \cdot 10^{12}\,\mathrm{cm}^{-2}$, there is a sufficient change in the resistive curves. Dependencies $R(H)$ become quasi-linear and, moreover, quasi-parallel for different temperatures T. This is most pronounced for even larger doses. For example, for the dose of $n_D = 7 \cdot 10^{12}\,\mathrm{cm}^{-2}$, typical resistive curves are shown in Fig. 9. As a result of this behavior of the dependences $R(H)$, the lines $H(T)$ do not almost change their slopes for different resistances R (see Fig. 10). It should be noted that the positive curvature near the critical temperature is exhibited here for rather low R compared to a virgin sample. In particularly for $n_D = 7 \cdot 10^{12}\,\mathrm{cm}^{-2}$, this appears at $R < 0.12R_N$. This allows a criterion to be formulated for the determination of $H_{c2}(T)$ in this case: $R^* = 0.12R_N$ for $n_D = 7 \cdot 10^{12}\,\mathrm{cm}^{-2}$. In figs. 7 and 10, we plot dependences $H_{c2}(T)$ by the solid blue lines for the virgin sample as well as for the film with $n_D = 7 \cdot 10^{12}\,\mathrm{cm}^{-2}$, respectively. Note that for larger doses, level R^* should be chosen even lower. The interpretation of this result is as follows. As n_D increases, the sample becomes more inhomogeneous. At high resistances, most of the film appears in a normal state and only local areas may participate in the non-dissipative flow of current. Therefore, the creep and flow of vortices only appears at the very bottom of the superconducting transition (when $R \approx 0$), when practically the entire film is in a superconducting state

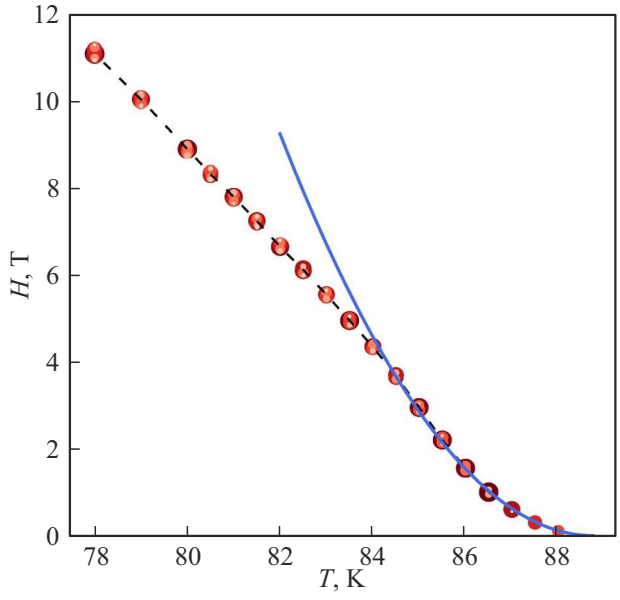

Figure 8. Experimental dependence $H(T)$ for $R = 0.02R_N$ (symbols) and $H(T) \propto (1 - T/T_{c0})^{3.2}$ dependence (solid line).

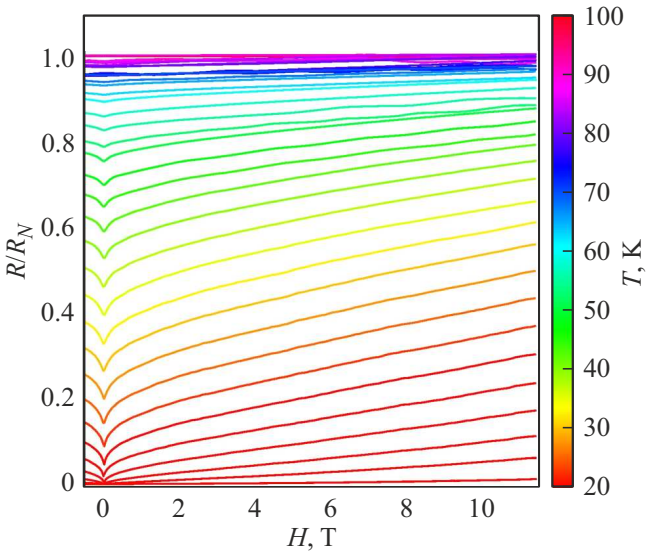

Figure 9. Experimental $R(H)/R_N$ curves for different T and $n_D = 7 \cdot 10^{12}\,\mathrm{cm}^{-2}$.

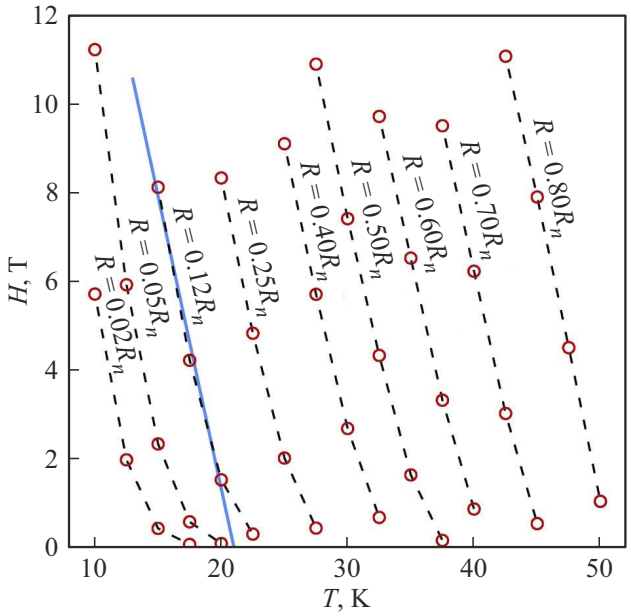

Figure 10. Dependencies $H(T)$ for different values of R/R_N and $n_D = 7 \cdot 10^{12}\,\mathrm{cm}^{-2}$. The symbols illustrate the experimental data and the dashed lines are obtained by spline interpolation. The solid blue line corresponds to a linear approximation over the set of experimental points represented by symbols for a given value R/R_N (the slope of this line corresponds to the slope of the critical field temperature dependence $H_{c2}(T)$).

and the dissipation is only determined by the movement of the vortices.

Note, that the experimental dependences $H_{c2}(T)$, determined within the proposed $R = R^*$ criterion, have insignificant deviations from the linear approximations shown by the solid blue lines in Figs. 7 and 10. These deviations are observed for substantially small magnetic fields H, close to zero. In other words, this occurs for temperatures near T_{c0}, when the so-called vortex liquid phase appears — vortex lattice melting occurs (see papers [18–20]). For HTSC, it is known that the vortex lattice melting is independent of the pinning potential in the case of materials with a weak disorder [21]. Therefore, it can be assumed that these deviations are related to the formation of the vortex fluid. We do not take them into account in our reasoning, as they are rather insignificant. Indeed, only one of each of the experimental points in Figs. 7 and 10 are outside the linear approximations represented by the solid blue lines.

5. Conclusion

In the present paper, we studied the specific features of superconducting transition broadening in YBCO epitaxial thin films with different doses of xenon irradiation. Based on Tinkham's model [13], we separated the vortex mechanism of broadening from other possible mechanisms. Thus, within the framework of our experimental studies it is found out that the phase transition line $H_{c2}(T)$ corresponds to a certain resistance $R = R^*$, which smoothly decreases from the value $0.4R_N$ for the virgin sample to practically zero value with a gradual increase in the defect concentration determined by the ion irradiation dose. The results of these studies appears to be rather important, since they allow to determine the value of the fundamental length scale in YBCO, the superconducting coherence length in the plane (ab), for the samples with an arbitrary defect concentration.

Acknowledgments

The authors thank A.S. Melnikov, V.V. Kurin and V.I. Gavrilenko for numerous discussions of the results, valuable advices, and recommendations. The authors are also grateful to V.K. Vasiljev and D.V. Guseinov for technical support in ion irradiation and E.V. Skorokhodov for his support in the diagnostics of the sample surface in SEM.

Funding

The study has been performed under the scientific program of the National Center for Physics and Mathematics, direction No. 6 „Nuclear and Radiation Physics“ as well as within the framework of the state assignment of the IPM RAS (theme GB: FFUF-2022-0006). The work was done using equipment of Center „Physics and technology of micro- and nanostructures“ at IPM RAS.

Conflict of interest

The authors declare that they have no conflict of interest.

References

[1] D. Saint-James, G. Sarma, E.J. Thomas. Type II Superconductivity, Pergamon, N.Y. (1969).
[2] T.R. Chien, T.W. Jing, N.P. Ong, Z.Z. Wang. Phys. Rev. Lett. **66**, 3075 (1991).
[3] J. Bardeen, M.J. Stephen. Phys. Rev. **140**, A1197 (1965).
[4] Ryusuke Ikeda. Phys. Rev. B **74**, 054510 (2006).
[5] A.I. Larkin, A.A. Varlamov. Theory of Fluctuations in Superconductors. Oxford University Press, N.Y. (2009).
[6] A. Zeinali, T. Golod, V.M. Krasnov. Phys. Rev. B **94**, 214506 (2016).
[7] A.A. Kopasov, D.A. Savinov, A.S. Mel'nikov. Phys. Rev. B, **95**, 104520 (2017).
[8] F. Hunte, J. Jaroszynski, A. Gurevich, D.C. Larbalestier, R. Jin, A.S. Sefat, M.A. McGuire, B.C. Sales, D.K. Christen, D. Mandrus. Nature (London) **453**, 903 (2008).
[9] J. Jaroszynski, F. Hunte, L. Balicas, Youn-jung Jo, I. Raicevic, A. Gurevich, D.C. Larbalestier, F.F. Balakirev, L. Fang, P. Cheng, Y. Jia, H.H. Wen. Phys. Rev. B **78**, 174523 (2008).
[10] Hyun-Sook Lee, Marek Bartkowiak, Jae-Hyun Park, Jae-Yeap Lee, Ju-Young Kim, Nak-Heon Sung, B.K. Cho, Chang-Uk Jung, Jun Sung Kim, Hu-Jong Lee. Phys. Rev. B **80**, 144512 (2009).
[11] M.A. Paalanen, A.F. Hebard, Appl. Phys. Lett. **45**, 794 (1984).
[12] E. Helfand, N.R. Werthamer. Phys. Rev. Lett. **13**, 686 (1964).
[13] M. Tinkham. Phys. Rev. Lett. **61**, 1658 (1988).
[14] A.V. Antonov, D.V. Masterov, A.N. Mikhaylov, S.V. Morozov, S.A. Pavlov, A.E. Parafin, D.I. Tetelbaum, S.S. Ustavschikov, P.A. Yunin, and D.A. Savinov. FTT **64**, *9*, 1162 (2022). (in Russian).
[15] J.F. Zeigler, J.P. Biersack, M.D. Zeigler. The Stopping and Range of Ions in Matter (SRIM). USA Chester Maryland (2008).
[16] U. Welp, W.K. Kwok, G.W. Crabtree, K.G. Vandervoort, J.Z. Liu. Phys. Rev. Lett. **30**, 4063 (1984).
[17] C. Xiaowen, W. Zhihe, Xu Xiaojun. Phys. Rev. B **65**, 064521 (2002).
[18] A. Houghton, R.A. Pelcovits, A. Sudbo. Phys. Rev. B **40**, 6763 (1989).
[19] E.H. Brandt. Phys. Rev. Lett. **63**, 1106 (1989).
[20] D.R. Nelson S. Seung. Phys. Rev. B **39**, 9153 (1989).
[21] V.M. Vinokur, M.V. Feigel'man, V.B. Geshkenbein, A.I. Larkin. Phys. Rev. Lett. **65**, 259 (1990).

Translated by Ego Translating